IJE TRANSACTIONS A: Basics Vol. 37 No. 04, (April 2024) 753-762

International Journal of Engineering

Journal Homepage: www.ije.ir

Seismic Assessment of Concrete Dams, Considering Anisotropy Caused by Lift Joints

R. Saeed*, A. J. Moradloo

Department of Civil Engineering, Faculty of Engineering, University of Zanjan, Zanjan, Iran

P A P E R I N F O

Paper history:
Received 21 August 2023
Received in revised form 02 November
Accepted 04 November 2023

Keywords:
Concrete Anisotropy
Lift Joints
Orthotropic Behavior
Concrete Gravity Dams
Seismic Loading

A B S T R A C T

Concrete dams are anisotropic due to lift joints that affect their performance. Lift joints are usually ignored in numerical analyses of concrete dams and the dam body is assumed to be homogeneous and isotropic. In this study, the seismic behavior of gravity dams was evaluated considering the anisotropy caused by lift joints, and the orthotropic and isotropic state responses were compared. Moreover, in the seismic loading range, a more detailed evaluation was done by applying the real effects of strain rate. Koyna concrete gravity dam was selected for the case study. The results showed that concrete anisotropy leads to larger dynamic displacements and greater damage to the dam body. By considering the orthotropic properties of concrete can lead to more realistic results. The maximum compressive and tensile stresses also increased in the anisotropic model compared to the homogeneous and isotropic model, indicating the usefulness of incorporating the orthotropic behavior of concrete in seismic analysis. In addition, considering the strain rate in the seismic loading range had an insignificant effect on the results. Therefore, considering the large dynamic increase factor in numerical analyses causes the error.

***doi**: 10.5829/ije.2024.37.04a.14*

Graphical Abstract

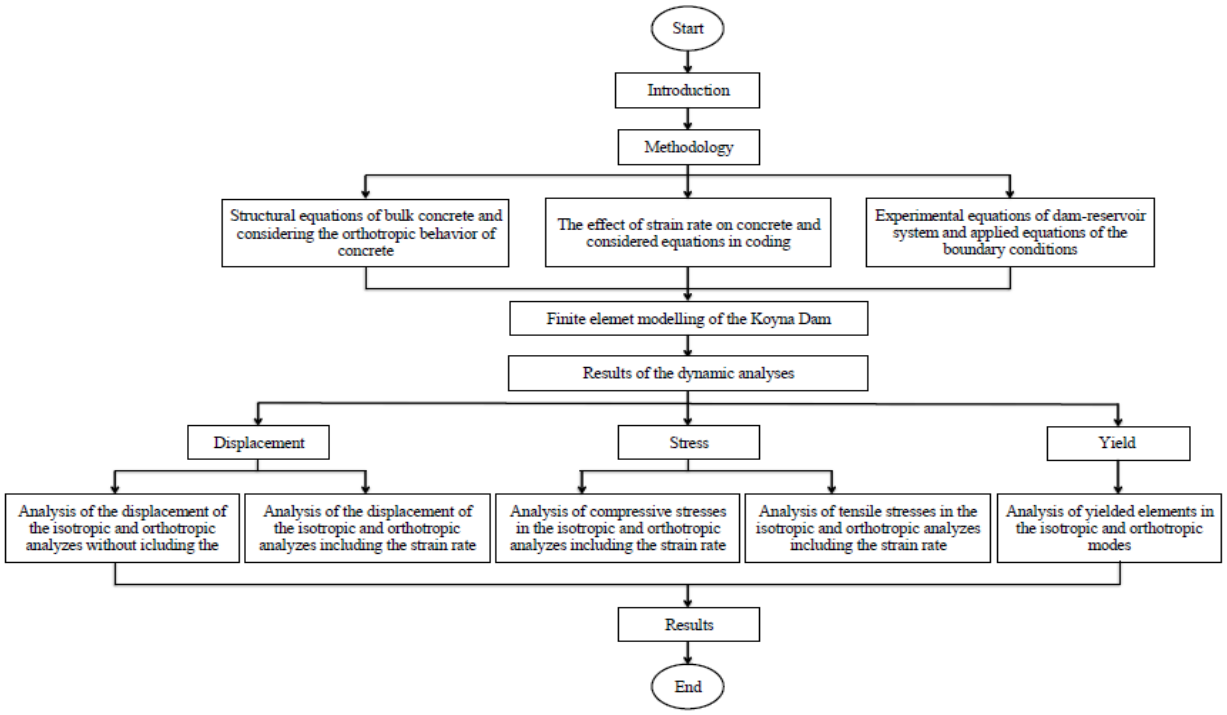

*Corresponding Author Email: Rezvan.saeed@znu.ac.ir (R. Saeed)

Please cite this article as: Saeed R, Moradloo AJ. Ash Seismic Assessment of Concrete Dams, Considering Anisotropy Caused by Lift Joints. International Journal of Engineering, A: Basics. 2024;37(04):753-62.

NOMENCLATURE

$d\sigma$	Stress increment	$d\varepsilon$	Strain increments
$[D]_0^{Orth}$	Orthotropic module matrix	$[D]_0^{Iso}$	Isotropic module matrix
E_i	Young's modulus	G_{ij}	Shear modulus
T	Rotation matrix	D	Material matrix
ν_{ij}	Poison's ratio	t	Time
$\dot{\varepsilon}$	Strain rate	ε	Strain
$CDIF$	Compressive DIF	$TDIF$	Tensile DIF
P	Hydrodynamic pressure in the reservoir	C	Sound propagation speed through fluid
$\vec{a}_{ns}$	Acceleration in the dam-reservoir interface	q	Admittance coefficient
n	Unit vector	$\ddot{v}_{gn}$	Ground acceleration
{R}	Matrix of ground motion effect on freedom degrees of structure nodes	α_b	Ratio of the reflected wave amplitude to the incident wave
$[M_s]$	Mass matrices of the structure	$[C_s]$	Damping matrices of the structure
$[K_s]$	Stiffness matrices of the structure	$[M_f]$	Mass matrices of fluid
$[C_f]$	Damping matrices of fluid	$[K_f]$	Stiffness matrices of fluid
{ä}	Acceleration vectors	{à}	Velocity vectors
{a}	Displacement vectors	Q	Dam-reservoir interaction matrix

1. INTRODUCTION

Dams are structures whose continuous evaluation is of great importance. Due to their large scale, experimental study of concrete dams is difficult and therefore, the numerical simulation is used in the dynamic analysis of such dams more effectively (1). To study the real behavior of these structures, acceptable modeling assumptions should be considered, and simplifying assumptions should be avoided. Based on the construction method of concrete dams, lift joints are inevitable. These joints cause weaker plates in the dam body that induce concrete anisotropy of the dam (2). While, in most studies, the dam body is considered homogenous and isotropic; however, these layers play an important role in the system response which leads to a more realistic response. Moreover, the strain rate is very influential in dynamic evaluation that should be evaluated in the seismic loading accurately and its real effects should be incorporated in the dynamic analyses. Ozturk (3) studied the effects of ground motion speed on the nonlinear displacement response of single degree of freedom (SDOF) systems and the relationship between the maximum nonlinear displacement response and the ground motion speed was evaluated. Fei and Gao (4) performed the dynamic analysis of concrete dams considering nonlinear materials. They developed a strain-dependent model to analyze the Koyna Gravity Dam and the Dagangshan Arch Dam. Based on the obtained results, different values of plastic strains were obtained using the models with and without considering strain rate, with the same distributions. Plastic deformations mainly occurred in areas with maximum tensile stress indicating tensile failure under seismic loads in these areas. Hesari et al. (5) studied the effect of contraction joints and lift joints on the seismic behavior of the Karoun 1 Arch Dam. The dam-reservoir-foundation system was modeled with and without joints, and the effect of contraction joints and lift joints on stress and displacement response under the effect of the earthquake was studied. According to the dynamic analysis results, considering the joints has a significant effect on the responses. By Hariri-Ardebili et al. (6) seismic evaluation of arch dams was investigated. Dez dam was chosen as the case study and all contraction and peripheral joints were modeled based on as-built drawings. Then, nonlinear seismic analysis of concrete arch dam–reservoir–foundation system considering joints behavior was investigated. The linear and nonlinear seismic analyses of concrete gravity dams were performed by Ouzandja and Tiliouine (7) and the effects of dam–foundation contact conditions on the seismic performance of the Oued Fodda concrete gravity dam were investigated. Alembagheri and Ghaemian (8) studied the seismic performance of arch concrete dams considering contraction joints using the ABAQUSE Software for the analysis of the Morrow-Point Dam case study considering three cases of integrated, three-joint, and seven-joint dam models. The results showed that incorporating contraction joints in the analysis had an insignificant effect on main tensile stresses, however, increased compressive stresses. In seismic analyses, an increase in the number of contraction joints generally decreased joint opening and sliding displacements. The opening of contraction joints changes the stress distribution in these structures and increases compressive stress which may result in concrete failure. Contraction joints can significantly decrease damage to the dam body and consequently, increase the seismic safety of the arch concrete dams. Yazdani and Alembagheri (9)studied the dynamic response of solid and cracked gravity dams. Pine Flat Dam was modeled considering a solid foundation and dam reservoir to study the effects of base joints and lift joints. Models of a solid dam, a dam with base joints, and a dam with base joints and two lift joints were developed and the results were compared. The structural stability and safety of the Pine Flat gravity dam located on an inhomogeneous rock foundation under the

static loads of self-weight, hydrostatic, and uplift pressure were evaluated by Ganji and Alembagheri (10). Latorre and Montans (11) presented a new theory for isotropic and anisotropic elastoplastic materials in large strains, which could be applied to elastoplastic metals and soft materials by incorporating strain rate as well. Lu et al. (12) studied the effects of heterogeneity on the nonlinear seismic response of concrete gravity dams and indicated that incorporating concrete heterogeneity can lead to higher damage to the concrete dams. Hai-tao et al. (13) numerically simulated the Koyna Dam under various seismic waves and studied the elastic-plastic seismic response of the Koyna Dam and the results of different scenarios were compared with actual damage to the dam. Ganji et al. (14) performed the seismic analysis of the Pine Flat gravity dam-reservoir-foundation system considering an inhomogeneous foundation. Different foundation characteristics were used and a heterogenic foundation was modeled. Assuming a homogeneous foundation results in a lower average of seismic responses. Hariri Ardebili (15) studied concrete heterogeneity by focusing on concrete dams and indicated that concrete heterogeneity affects progressive failure analysis and therefore, should be included in risk assessments. It was also indicated that crack propagation in macro-heterogeneous materials may differ from homogeneous ones. Therefore, it becomes more important in the case of concrete gravity dams which are more susceptible to heterogeneity due to construction limitations. Guo et al. (16) studied the seismic response of the arch dam considering the vertical and shear joints. The results showed a significant effect of joints on the stress distribution in the nonlinear model, with a significantly increased maximum main tensile stress. Lee and Kwak (17) proposed a strain rate-dependent orthotropic model for reinforced concrete with steel fiber subjected to impact or blast loads. The improved model was an orthotropic model introduced by the same author for plain concrete. Then, the model was analyzed using Ls-Dyna numerical model. The model has minimal dependence on mesh size and can be developed by adding different concrete parameters. Pan (18) developed a complete model of the dam system, foundation, and reservoir to study the effect of concrete heterogeneity on the seismic response of the dam. The Weibull probabilistic distribution assumption was used to define concrete heterogeneity. The results showed that concrete heterogeneity significantly influences the seismic damage to the concrete gravity dams. Lu et al. (19) evaluated damage to the concrete gravity dams considering the heterogeneity of concrete tensile strength and indicated that the possibility of failure increased. Liu et al. (20) studied the effects of concrete heterogeneity on the nonlinear seismic response of concrete gravity dams under different earthquakes. The ABAQUS Software was used to model the Koyna Dam and to include strain rate, dynamic resistance was assumed 20% higher than the static resistance. The uncertainty of seismic responses and damage patterns were quantified, and the correlation effect between the module and concrete strength was studied. It was concluded that there were significant differences between seismic responses of the homogenous and heterogeneous models, and ignoring the concrete heterogeneity can result in an incorrect estimation of damage pattern to the concrete gravity dams, and the effects of concrete heterogeneity on the nonlinear dynamic response of concrete dams are highly dependent on the input seismic motions. Kadhim et al. (21) studied the behavior of cracked arched concrete dam under moderate intensity earthquake experimentally as well as by using nonlinear analyses. The extended finite element method (XFEM) was described for crack propagation. Li et al. (22) performed a fuzzy analysis of the seismic fragility of gravity dams. Due to different concrete strengths at different dam locations caused by concreting process and concrete heterogeneity, they proposed a method for fuzzy-seismic analysis of dams incorporating local changes in material properties. In this case, the damage to the dam body is intensified which is accompanied by an increase in the number and depth of cracks. They reported that ignoring concrete heterogeneity can lead to an underestimation of the seismic fragility of concrete gravity dams. It can be concluded that, in the construction of gravity dams, the quality of concreting process should be thoroughly observed to reduce local changes in concrete strength. Due to significant financial, fatal and environmental damages, high importance structures are expected to continue their performance after the earthquake. As a result, more research on the seismic performance of these structures is required to achieve their highest level of earthquake resistance (23). In addition, by knowing the behavior of the structure and analyzing it accurately, it is possible to build new structures as well as repair, reconstruct, renovate and retrofit existing structures (24). Based on the technical literature, it is observed that assuming concrete homogeneity and isotropy leads to incorrect results in seismic analyses. Therefore, this has been taken into account in recent evaluations. In many studies, a few layers in the dam height have been modeled to include lift joints. Although the layers are located in sensitive areas in numerical modeling and are determined based on crack profiles of nonlinear seismic finite element analysis, however, there are intermittent lift joints throughout the dam height with different concrete properties. So, modeling based on a limited number of layers is erroneous and despite accurate modeling of the layers, it is accompanied by approximation due to dealing with anisotropic materials. Therefore, lift joints, which are weaker plates with different characteristics than concrete and are alternately present throughout the dam height. Considering limited few lift joints in the dam

height causes errors and leads to incorrect results. Therefore, in the present study, for more accurate modeling, orthotropic material was used to include the lift joints and the mechanical behavior of concrete in the direction perpendicular to the lift joints was considered different from that of the horizontal planes. On the other hand, considering the effect of strain rate in dynamic loading, in the present study, using experimental equations and taking into account the real effects of strain rate in the seismic loading range, strain rate was included in a more precise way in modeling. Therefore, in order to have a more accurate modeling, the effects of loading rate and strain rate were studied. The Finite Element Method (FEM) is widely adopted due to its ability to deal with heterogeneous and anisotropic materials and complex boundaries (25). In the present study, the required elements and subroutines were added to the FEAPpv finite-element model, and a new program called GFEAP was developed. Then, the dynamic behavior of the Koyna Gravity Dam was studied using the developed finite-element numerical model. The geometrical input models, assembling matrices, and solver vectors of the original numerical model were used and a three-dimensional 20-node serendipity element as well as a 20-node fluid element were added to the numerical model. Moreover, by adding the required sub-routines, the behavior of the concrete gravity dam under seismic loading was analyzed considering strain rate effects and orthotropic concrete properties.

2. METHODOLOGY

2. 1. Structural Relationship of Mass Concrete

The overall stress-strain equation can be expressed as follows (26-28):

$$d\sigma = D_0\, d\varepsilon \tag{1}$$

where dσ and dε are stress and strain increments, respectively. In the anisotropic case, the module matrix, $[D]_0^{Orth}$, is defined as follows:

$$[D]_0^{Orth} = \frac{1}{\Omega}\begin{bmatrix} E_1(1-\nu_{23}\nu_{32}) & E_1(\nu_{21}+\nu_{23}\nu_{31}) & E_1(\nu_{31}+\nu_{21}\nu_{32}) & 0 & 0 & 0 \\ E_2(\nu_{12}+\nu_{13}\nu_{32}) & E_2(1-\nu_{13}\nu_{31}) & E_2(\nu_{32}+\nu_{12}\nu_{31}) & 0 & 0 & 0 \\ E_3(\nu_{13}+\nu_{12}\nu_{23}) & E_3(\nu_{23}+\nu_{13}\nu_{21}) & E_3(1-\nu_{12}\nu_{21}) & 0 & 0 & 0 \\ 0 & 0 & 0 & G_{12}\Omega & 0 & 0 \\ 0 & 0 & 0 & 0 & G_{23}\Omega & 0 \\ 0 & 0 & 0 & 0 & 0 & G_{31}\Omega \end{bmatrix} \tag{2}$$

where

$$\Omega = 1-\nu_{21}\nu_{12}-\nu_{31}\nu_{13}-\nu_{32}\nu_{23}-\nu_{12}\nu_{23}\nu_{31}-\nu_{21}\nu_{32}\nu_{13} \tag{3}$$

In the above matrix, ν_{ij} is Poison's ratio (i. j = 1.2.3), E_i is Young's modulus in the direction i (i = 1.2.3), and G_{ij} is shear modulus in plane i − j (i. j = 1.2.3) and is calculated as follows:

$$G_{ij} = \frac{E_i E_j}{E_i(1+\nu_{ij})+E_j(1+\nu_{ji})} \tag{4}$$

By taking into account the effect of lift joints under static and dynamic loads, the material properties can be assumed isotropic in two horizontal directions, and new concrete properties in a direction perpendicular to lift joints can be defined. As a result (2):

$$\frac{\nu_{12}}{E_1}=\frac{\nu_{21}}{E_2};\ \frac{\nu_{13}}{E_1}=\frac{\nu_{31}}{E_3};\ \frac{\nu_{23}}{E_2}=\frac{\nu_{32}}{E_3} \tag{5}$$

For isotropic materials (29, 30):

$$E_1 = E_1 = E_1 = E.\ \nu_{12}=\nu_{13}=\nu_{23}=\nu.$$
$$G_{12}=G_{13}=G_{23}=G \tag{6}$$

The isotropic module matrix, $[D]_0^{Iso}$, is as follows (29):

$$[D]_0^{Iso} = \frac{E}{(1+\nu)(1-2\nu)}\begin{bmatrix} 1-\nu & \nu & \nu & 0 & 0 & 0 \\ \nu & 1-\nu & \nu & 0 & 0 & 0 \\ \nu & \nu & 1-\nu & 0 & 0 & 0 \\ 0 & 0 & 0 & \frac{1-2\nu}{2} & 0 & 0 \\ 0 & 0 & 0 & 0 & \frac{1-2\nu}{2} & 0 \\ 0 & 0 & 0 & 0 & 0 & \frac{1-2\nu}{2} \end{bmatrix} \tag{7}$$

In finite element settings, the incremental stress-strain equation should be converted to a global reference system taking into account orthotropic axes. This can be achieved by using the rotation matrix, T, as follows (26):

$$D = T^T D_0 T \tag{8}$$

where D is the material matrix of the overall coordinate system.

2. 2. The Effect of Strain Rate on Concrete

To include the effect of strain rate, the empirical dynamic increase coefficients were used (31). For this purpose, the strain obtained at each time step was used to calculate the strain rate. Then, using the empirical DIF equations, the dynamic increase factor for each time step was calculated and applied.

$$\dot{\varepsilon} = \frac{d\varepsilon}{dt} \quad (9)$$

where $\dot{\varepsilon}$ is the strain rate, ε is strain, and t is time. According to extensive experimental studies by Hao et al. (32), the compressive and tensile DIF equations considered for concrete, based on which the encoding was performed, are as follows (31):

$$CDIF = 0.0419(\log\dot{\varepsilon}) + 1.2165 \; for \; \dot{\varepsilon} \leq {}^{30}/_{S} \quad (10)$$

$$CDIF = 0.8988(\log\dot{\varepsilon})^2 - 2.8255(\log\dot{\varepsilon}) + 3.4907 \; for \; {}^{30}/_{S} < \dot{\varepsilon} \leq {}^{1000}/_{S} \quad (11)$$

$$TDIF = 0.26(\log\dot{\varepsilon}) + 2.06 \; for \; \dot{\varepsilon} \leq {}^{1}/_{S} \quad (12)$$

$$TDIF = 2(\log\dot{\varepsilon}) + 2.06 \; for \; {}^{1}/_{S} < \dot{\varepsilon} \leq {}^{2}/_{S} \quad (13)$$

$$TDIF = 1.44331(\log\dot{\varepsilon}) + 2.2276 \; for \; {}^{2}/_{S} < \dot{\varepsilon} \leq {}^{150}/_{S} \quad (14)$$

The calculated dynamic increase factor is multiplied by the static yield surface to increase the dynamic strength of the structure compared to the static strength and therefore, the dynamic increase factor is applied to the constitutive model.

2. 3. Theoretical Equations of Dam-Reservoir System By assuming a homogeneous, isotropic, non-viscous, and non-rotational fluid, then the governing equation on hydraulic pressure wave propagating in the reservoir (Helmholtz Equation) is as follows (33-37):

$$\nabla^2 P = \frac{1}{C^2}\frac{\partial^2 P}{\partial t^2} \quad (15)$$

where $P(x.y.z.t)$ is the hydrodynamic pressure in the reservoir, and C and t are the sound propagation speed through fluid and time variables, respectively. To solve the above equation for the reservoir, appropriate boundary conditions should be applied, as described in the following.

Dam-Reservoir Interface: Because of the same normal fluid and structure velocities in this interface, the boundary condition is expressed as follows:

$$\rho\vec{a}_{ns} = -\frac{\partial P}{\partial n} \quad (16)$$

where $\vec{a}_{ns}$ is the acceleration in the dam-reservoir interface perpendicular to the dam, ρ is the volumetric mass of the fluid, P is the hydrodynamic pressure, and n is the unit vector perpendicular to the dam surface inwards the reservoir.

Reservoir-Foundation Interface: On this surface, due to bed floor sedimentation and sediment properties, a part of the wave energy hitting the bed floor is absorbed and a part is reflected. In this boundary, the following equation is met:

$$\frac{\partial P}{\partial n} = -\rho\ddot{v}_{gn} - q\frac{\partial P}{\partial t} \; ; \; q = \frac{1}{C}\left(\frac{1-\alpha_b}{1+\alpha_b}\right) \quad (17)$$

where $\ddot{v}_{gn}$ is the ground acceleration element perpendicular to the boundary, q is the admittance or damping coefficient on the reservoir floor which is expressed as above using α_b, and α_b is the ratio of the reflected wave amplitude to the incident wave.

Upstream Reservoir Boundary: By assuming a considerable reservoir length, the following equation can be used for this boundary:

$$\frac{\partial P}{\partial n} = -\frac{1}{C}\frac{\partial P}{\partial t} \quad (18)$$

The physical interpretation of Equation 18 is that a group of dampers is installed in the upstream reservoir boundary.

Free Surface of the Reservoir: The surface waves are commonly ignored in tall dams and consequently, the boundary condition of the reservoir's free surface is obtained as follows:

$$P = 0 \quad (19)$$

Considering the static response of the dam-reservoir system as an initial condition, the dam-reservoir system interaction equation for the dynamic response of the system under earthquake is obtained as follows (22, 28, 38, 39):

$$\begin{bmatrix} M_s & 0 \\ \rho Q^T & M_f \end{bmatrix}\begin{Bmatrix} \ddot{a} \\ \ddot{P} \end{Bmatrix} + \begin{bmatrix} C_s & 0 \\ 0 & C_f \end{bmatrix}\begin{Bmatrix} \dot{a} \\ \dot{P} \end{Bmatrix} + \begin{bmatrix} K_s & Q \\ 0 & K_f \end{bmatrix}\begin{Bmatrix} a \\ P \end{Bmatrix} + \begin{Bmatrix} M_s\{R\} & \{\ddot{u}g\} \\ \rho Q^T\{R\} & \{\ddot{u}g\} \end{Bmatrix} = 0 \quad (20)$$

where $[M_s]$, $[C_s]$, and $[K_s]$ are the mass, damping, and stiffness matrices of the structure, respectively. $[M_f]$, $[C_f]$ and $[K_f]$ are the mass, damping, and stiffness matrices of fluid, respectively; and $\{\ddot{a}\}$, $\{\dot{a}\}$, and $\{a\}$ are acceleration, velocity, and displacement vectors, respectively; and $\{P\}$, $\{\dot{P}\}$, and $\{\ddot{P}\}$ are hydrodynamic pressure, first-order and second-order derivatives of hydrodynamic pressure, respectively. In addition, $\{R\}$ is the matrix of ground motion effect on freedom degrees of structure nodes, $\{\ddot{u}g\}$ is the vector of gravity acceleration components in the directions of the coordinate system, Q is the dam-reservoir interaction matrix, and ρ is the volumetric mass of the fluid.

3. FINITE-ELEMENT MODELING OF THE KOYNA DAM

In the present study, sub-routines were written in Fortran and added to the FEAPpv finite-element numerical model which was called GFEAP. A 20-node 3D serendipity element and a 20-node 3D fluid element with pressure degrees of freedom were added to the numerical

model and used in the modeling. Moreover, sub-routines of the dam-reservoir dynamic interaction using the staggered method, the five-parameter William-Warnke plasticity model as well as a sub-routine for calculation and application of dynamic increase factor were also added to the numerical model (40). The Koyna dam was selected as the case study, which is a concrete gravity dam with a height of 103 m and a foundation width of 70.2 m constructed in India. A 2D model of the dam along with its reservoir (with a length twice the dam height) was developed and a staggered problem-solving pattern was used to solve the dam-reservoir interaction equations. Foundation modelling as well as foundation-structure interaction were ignored. The weight and hydrostatic pressure static loads were applied and used as initial responses in dynamic analyses. The dam body was modeled using 72 three-dimensional brick elements and 592 nodes. Figure 1 shows the finite element mesh of the dam. To show the effect of earthquake on the response of structures, it is necessary to use the time history of earthquake. Earthquake vibration data is required for the design of tall buildings or large-scale structures such as dams or bridges (41). In the present paper, the vertical and horizontal components of the Taft Earthquake were used in dynamic analyses of the Koyna Dam, as shown in Figures 2 and 3. The compressive strength of concrete used in dam construction was 20.4 MPa with a tensile strength of 2 MPa. The concrete density was $2640\ \mathrm{kg/m^3}$, sound speed in water was $1440\ \mathrm{m/s}$, and the impedance ratio of the abutments was assumed as 3.44. In the isotropic state, Young's modulus and Poisson's ratio were considered as 26.35 GPa and 0.2, respectively. Considering different concrete properties in a direction perpendicular to joints (compared to other directions) and assuming an anisotropy ratio of 1.2, Young's modulus in the vertical direction was calculated as 21.8 GPa (15).

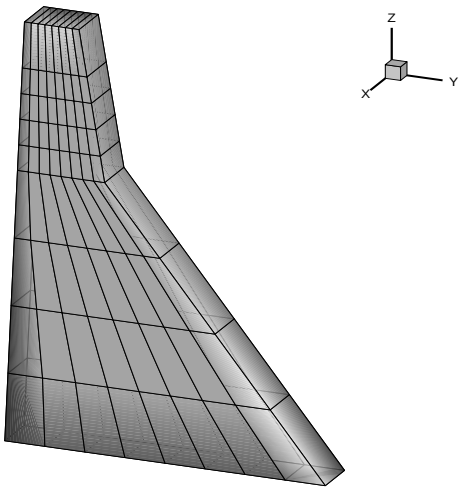

Figure 1. Finite-Element Mesh of the Koyna Dam Body

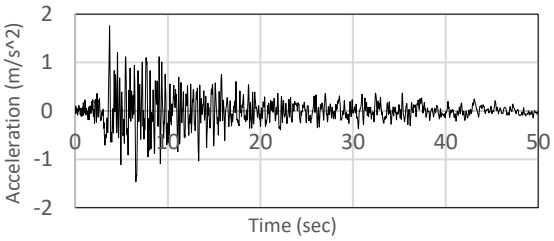

Figure 2. Horizontal Component of the Taft Earthquake

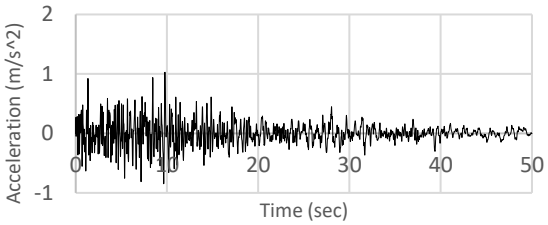

Figure 3. Vertical Component of the Taft Earthquake

4. RESULTS OF DYNAMIC ANALYSIS

To study the lift joints, isotropic and orthotropic analyses were performed incorporating the strain rate of the Koyna dam. The time history of a point located on the dam crest in river (longitudinal) directions for the isotropic and orthotropic states considering strain rate is shown in Figure 4. The positive displacement direction is toward downstream. The maximum displacements of the dam crest in the river direction for the isotropic and orthotropic states were 2.32 cm and 2.9 cm, respectively. In the above states, the maximum static displacements in the longitudinal direction were 0.51 cm and 0.61 cm, respectively. The maximum displacements in the dam height (vertical) direction for the isotropic and orthotropic states were 0.64 cm and 0.81 cm, respectively. Considering lift joints and orthotropic state compared to the homogeneous and isotropic state leads to an increase of 24.88% and 25.59% in the longitudinal and vertical directions, respectively. Displacement envelope in the isotropic and orthotropic states considering strain rate is shown in Figures 5 and 6. As can be seen, a similar pattern is observed. The results of the isotropic and orthotropic states were compared without including strain rate and to study the effect of loading rate, the results were compared with the obtained results considering strain rate. The time history of dam crest displacement in the river direction for the isotropic and orthotropic analyses without including strain rate is presented in Figure 7. The maximum displacements in the longitudinal direction for the isotropic and orthotropic states were 2.3223 cm and 2.9015 cm, respectively. Negligible differences occurred with and without considering the strain rate. Using the orthotropic

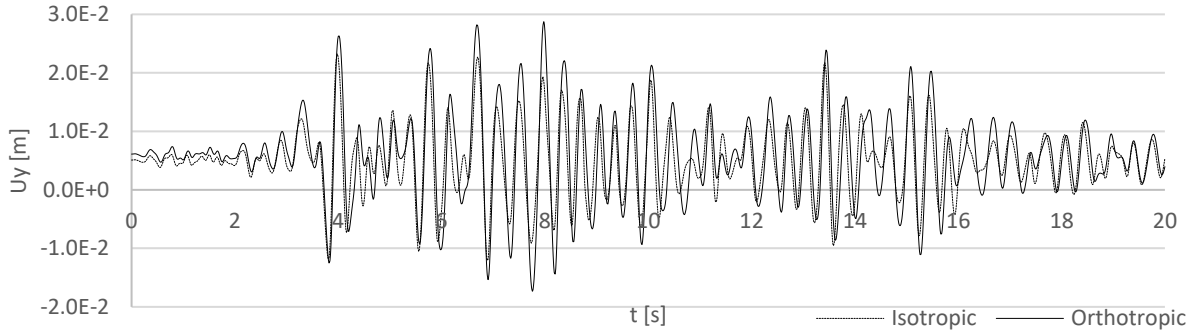

Figure 4. Displacement time history at the midpoint of the dam crest in the longitudinal direction for the isotropic and orthotropic analyses considering strain rate

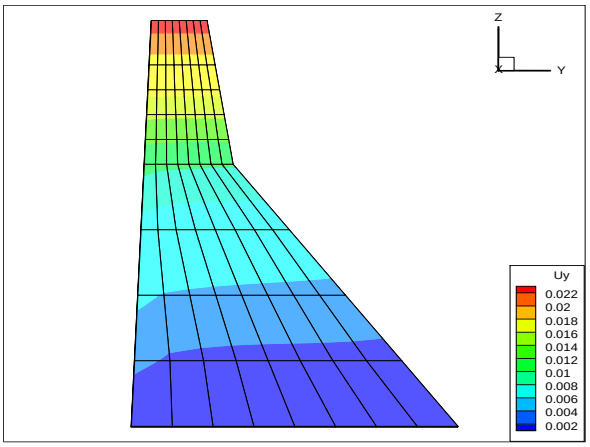

Figure 5. Dam Displacement envelope in the Longitudinal Direction for the Isotropic analyses without considering the strain rate

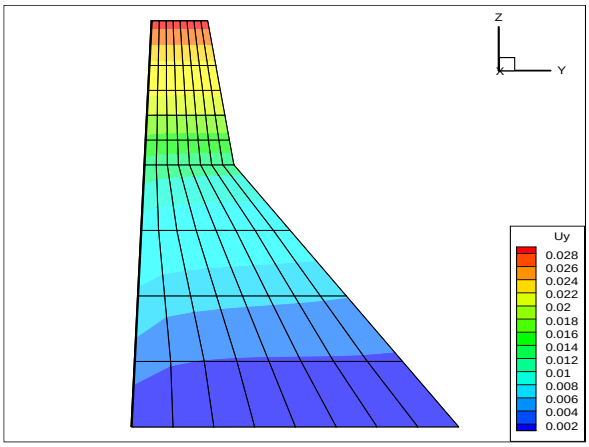

Figure 6. Dam Displacement envelope in the longitudinal Direction for the Orthotropic analyses without considering the strain rate

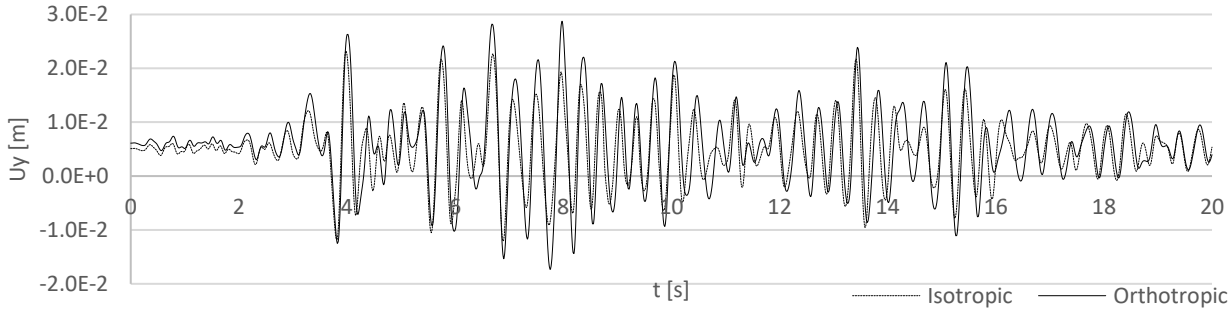

Figure 7. Displacement time history at the midpoint of the dam crest in the longitudinal direction for the isotropic and orthotropic analyses without considering the strain rate

state an increase of 24.94% and 25.66% was observed compared to the isotropic one in the longitudinal and vertical directions, respectively. A negligible difference between distribution patterns and values of the displacement envelope was observed with and without considering the strain rate and therefore, is not presented here. The envelope of principal maximum (tensile) and minimum (compressive) stresses on the upstream side of the dam body in the orthotropic and isotropic analyses including the strain rate are represented in Figures 8 to 11, respectively. As can be seen from Figures 8 and 9, maximum tensile stress in the isotropic and orthotropic states occurred in the dam neck and dam heel. The same distribution pattern was observed in both cases, however, in the orthotropic state a wider distribution occurred throughout the dam body. Maximum tensile stresses in

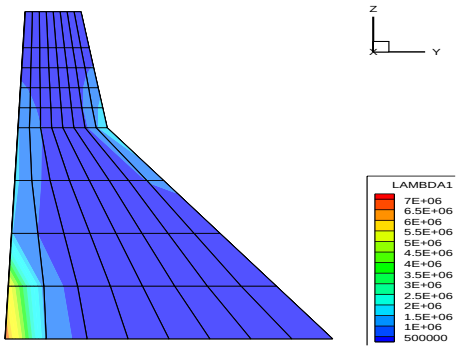

Figure 8. Maximum principal stress (Tensile) envelope in the isotropic state

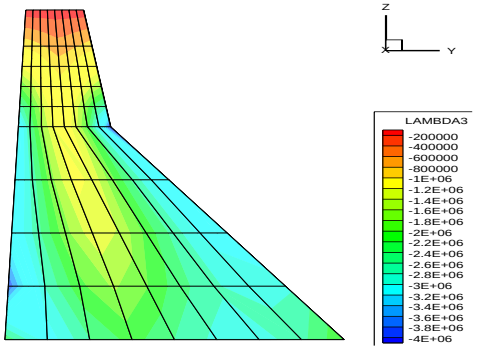

Figure 9. Minimum principal stress (Compressive) envelope in the isotropic state

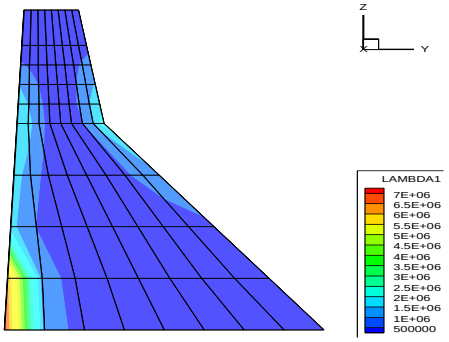

Figure 10. Maximum principal stress (Tensile) envelope in the orthotropic state

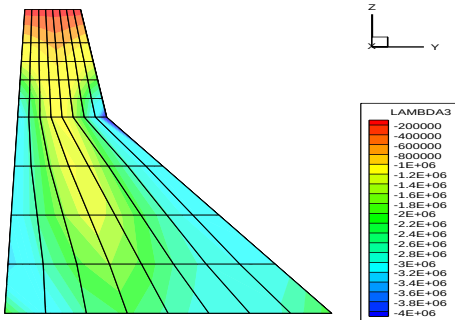

Figure 11. Minimum principal stress (Compressive) envelope in the orthotropic state

the isotropic and orthotropic states were 7.10E+0 Pa and 7.26E+06 Pa, respectively, indicating an increase of 2.34 percent. Maximum compressive stress in the isotropic and orthotropic states occurred in downstream and dam neck with values of -4.14E+06 Pa and 4.26E+06 Pa in the isotropic and orthotropic states, respectively, indicating an increase of 2.78 percent.

The damaged areas of the dam reflect the weak locations. As can be seen, in the isotropic and orthotropic models, the yield function was equal to 0.075 and 0.095, respectively. The yield area is the same as the location with the main tensile stress in the models and in both states, yield areas are focused in the dam heel and slope-changing area in downstream. Yield areas are the same in both the isotropic and orthotropic states with a wider distribution in the orthotropic state. The damaged areas correspond to the tensile stress envelope and the location of maximum tensile stress. Figures 12 and 13 show the yielded areas in both states.

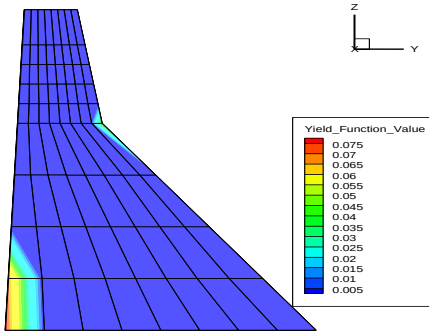

Figure 12. Yielded elements envelope in the isotropic state

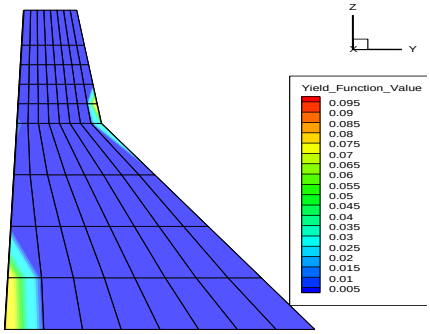

Figure 13. Yielded elements envelope in the orthotropic state

5. CONCLUSIONS

In the present paper, based on precise empirical relations of dynamic increase factor, the real effect of strain rate in the seismic loading range on the Koyna concrete gravity dam was studied. Lift joints were also taken into account by applying orthotropic concrete properties

perpendicular to the lift joints. Based on the analyses, the following results were obtained:

1. Obtained displacements in the case of including strain rate were smaller than without strain rate, however, the difference was insignificant so that the strain rate effect can be neglected in seismic loading. Consequently, using large dynamic increase coefficients can lead to errors in the seismic analyses.
2. The time histories of the isotropic and orthotropic models had insignificant differences, however, incorporating anisotropy due to lift joints results in more accurate results. As mentioned before, considering lift joints led to an increase of about 25% in displacements compared to the isotropic model.
3. Tensile and compressive stresses in the orthotropic material state were higher than those in the isotropic one, however, the same distribution pattern was observed. Maximum tensile stress occurred in the dam heel and neck, which are susceptible to damage.
4. A similar damage pattern was observed in the isotropic and anisotropic models with a wider distribution in the orthotropic model. Therefore, ignoring concreting layer can lead to damage underestimation.

6. REFERENCES

1. Davani Motlagh A, Sadeghian M, Javid A, Asgari M. Optimization of dam reservoir operation using grey wolf optimization and genetic algorithms (A case study of Taleghan Dam). International Journal of Engineering. 2021;34(7):1644-52. 10.5829/IJE.2021.34.07A.09
2. Puzrin A. Constitutive modelling in geomechanics: introduction: Springer Science & Business Media; 2012.
3. Ozturk B. Investigation of effects of ground motions on SDOF systems using records from the recent earthquakes in Turkey. New Horizons and Better Practices2007. p. 1-8.
4. Fei L, Gao L. Application of thermodynamics-based rate-dependent constitutive models of concrete in the seismic analysis of concrete dams. Water Science and Engineering. 2008;1(3):54-64. https://doi.org/10.3882/j.issn.1674-2370.2008.03.006
5. Hesari MA, Ghaemian M, Shamsai A. Advanced nonlinear dynamic analysis of arch dams considering joints effects. Advances in Mechanical Engineering. 2014;6:587263. https://doi.org/10.1155/2014/587263
6. Hariri-Ardebili M, Mirzabozorg H, Estekanchi H. Nonlinear seismic assessment of arch dams and investigation of joint behavior using endurance time analysis method. Arabian Journal for Science and Engineering. 2014;39:3599-615. https://doi.org/10.1007/s13369-014-1027-5
7. Ouzandja D, Tiliouine B. Effects of Dam–Foundation Contact Conditions on Seismic Performance of Concrete Gravity Dams. Arabian Journal for Science and Engineering. 2015;40:3047-56. https://doi.org/10.1007/s13369-015-1770-2
8. Alembagheri M, Ghaemian M. Seismic performance evaluation of a jointed arch dam. Structure and Infrastructure Engineering. 2016;12(2):256-74. https://doi.org/10.1080/15732479.2015.1009124
9. Yazdani Y, Alembagheri M. Effects of base and lift joints on the dynamic response of concrete gravity dams to pulse-like excitations. Journal of Earthquake Engineering. 2017;21(5):840-60. https://doi.org/10.1080/13632469.2016.1185056
10. Ganji HT, Alembagheri M. Stability of monolithic gravity dam located on heterogeneous rock foundation. Arabian Journal for Science and Engineering. 2018;43:1777-93. https://doi.org/10.1007/s13369-017-2755-0
11. Latorre M, Montans FJ. A new class of plastic flow evolution equations for anisotropic multiplicative elastoplasticity based on the notion of a corrector elastic strain rate. Applied Mathematical Modelling. 2018;55:716-40. https://doi.org/10.1016/j.apm.2017.11.003
12. Lu X, Wu Z, Pei L, He K, Chen J, Li Z, et al. Effect of the spatial variability of strength parameters on the dynamic damage characteristics of gravity dams. Engineering Structures. 2019;183:281-9. https://doi.org/10.1016/j.engstruct.2019.01.042
13. Hai-tao W, Jiayu S, Feng W, Zhiqiang A, Tianyun L. Experimental study on elastic-plastic seismic response analysis of concrete gravity dam with strain rate effect. Soil Dynamics and Earthquake Engineering. 2019;116:563-9. https://doi.org/10.1016/j.soildyn.2018.09.020
14. Ganji HT, Alembagheri M, Khaneghahi MH. Evaluation of seismic reliability of gravity dam-reservoirinhomogeneous foundation coupled system. Frontiers of Structural and Civil Engineering. 2019;13:701-15. https://doi.org/10.1007/s11709-018-0507-1
15. Hariri-Ardebili MA. Uncertainty quantification of heterogeneous mass concrete in macro-scale. Soil Dynamics and Earthquake Engineering. 2020;137:106137. https://doi.org/10.1016/j.soildyn.2020.106137
16. Guo S, Liao J, Huang H, Liang H, Li D, Chen H, et al. The effect of shear sliding of vertical contraction joints on seismic response of high arch dams with fine finite element model. Advances in Civil Engineering. 2020;2020. https://doi.org/10.1155/2020/4353609
17. Lee M, Kwak H-G. A strain rate dependent nonlinear elastic orthotropic model for SFRC structures. Journal of Building Engineering. 2021;42:102466. https://doi.org/10.1016/j.jobe.2021.102466
18. Pan J. Seismic damage behavior of gravity dams under the effect of concrete inhomogeneity. Journal of Earthquake Engineering. 2021;25(7):1438-58. https://doi.org/10.1080/13632469.2019.1581675
19. Lu X, Pei L, Chen J, Wu Z, Li Z. Comparison of homogenous and random fields of tensile strength effects on the nonlinear dynamical response of Guandi concrete gravity dams under strong earthquake waves. Structure and Infrastructure Engineering. 2021;17(12):1684-97. https://doi.org/10.1080/15732479.2020.1832534
20. Liu P, Chen J, Fan S, Xu Q, editors. Uncertainty quantification of the effect of concrete heterogeneity on nonlinear seismic response of gravity dams including record-to-record variability. Structures; 2021: Elsevier.
21. Kadhim M, Alfatlawi T, Hussein M. Experimental and nonlinear analysis of cracking in concrete arch dams due to seismic uplift pressure variations. International Journal of Engineering, Transactions B: Applications. 2021;34(5):1156-66. http://10.5829/IJE.2021.34.05B.09
22. Li Z, Wu Z, Chen J, Pei L, Lu X. Fuzzy seismic fragility analysis of gravity dams considering spatial variability of material parameters. Soil Dynamics and Earthquake Engineering. 2021;140:106439. https://doi.org/10.1016/j.soildyn.2020.106439
23. Saria A, Djermane M, Hadj-Djelloul ND. Three-Dimensional Nonlinear Dynamic Analysis of Base Isolated Cylindrical Steel Tank. Civil Engineering Journal. 2022;8(06). http://dx.doi.org/10.28991/CEJ-2022-08-06-013

24. Balamuralikrishnan R, Al-Mawaali A, Al-Yaarubi M, Al-Mukhaini B, Kaleem A. Seismic upgradation of RC beams strengthened with externally bonded spent catalyst based ferrocement laminates. HighTech and Innovation Journal. 2023;4(1):189-209. https://10.28991/HIJ-2023-04-01-013
25. Fadaei-Kermani E, Shojaee S, Memarzadeh R. Numerical Simulation of Seepage Flow through Dam Foundation Using Smooth Particle Hydrodynamics Method (RESEARCH NOTE). International Journal of Engineering, Transactions A: Basics. 2019;32(4):484-8. http://10.5829/IJE.2019.32.04A.04
26. Balan TA, Spacone E, Kwon M. A 3D hypoplastic model for cyclic analysis of concrete structures. Engineering Structures. 2001;23(4):333-42. https://doi.org/10.1016/S0141-0296(00)00048-1
27. Bono G, Campos Filho A, Pacheco A. Modelo 3D de elementos finitos para análise de estruturas de concreto armado. Revista IBRACON de Estruturas e Materiais. 2011;4:548-60. https://doi.org/10.1590/S1983-41952011000400002
28. Wei K, Chen S, Li G, Han H. Application of a generalised plasticity model in high earth core dam static and dynamic analysis. European Journal of Environmental and Civil Engineering. 2020;24(7):979-1012. https://doi.org/10.1080/19648189.2018.1437777
29. Hariri-Ardebili M, Mirzabozorg H. Orthotropic material and anisotropic damage mechanics approach for numerically seismic assessment of arch dam–reservoir–foundation system. Strength of Materials. 2013;45:648-65. https://doi.org/10.1007/s11223-013-9501-y
30. Penado FE. Fracture parameter determination for the orthotropic interface crack with friction. Engineering Fracture Mechanics. 2018;204:542-56. https://doi.org/10.1016/j.engfracmech.2018.10.038
31. Ye Z, Hao Y, Hao H. Numerical study of the compressive behavior of concrete material at high strain rate with active confinement. Advances in Structural Engineering. 2019;22(10):2359-72. https://doi.org/10.1177/1369433219841174
32. Hao Y, Hao H, Li Z. Influence of end friction confinement on impact tests of concrete material at high strain rate. International journal of impact engineering. 2013;60:82-106. https://doi.org/10.1016/j.ijimpeng.2013.04.008
33. Cetin M, Mengi Y. Transmitting boundary conditions suitable for analysis of dam-reservoir interaction and wave load problems. Applied Mathematical Modelling. 2003;27(6):451-70. https://doi.org/10.1016/S0307-904X(03)00048-9
34. Omidi O, Lotfi V. A symmetric implementation of pressure-based fluid–structure interaction for nonlinear dynamic analysis of arch dams. Journal of Fluids and structures. 2017;69:34-55. https://doi.org/10.1016/j.jfluidstructs.2016.12.003
35. Sharma V, Fujisawa K, Murakami A. Space–time FEM with block-iterative algorithm for nonlinear dynamic fracture analysis of concrete gravity dam. Soil Dynamics and Earthquake Engineering. 2020;131:105995. https://doi.org/10.1016/j.soildyn.2019.105995
36. Moradloo AJ, Naiji A. Effects of rotational components of earthquake on seismic response of arch concrete dams. Earthquake Engineering and Engineering Vibration. 2020;19:349-62. https://doi.org/10.1007/s11803-020-0566-x
37. Varmazyari M, Sabbagh-Yazdi S-R. Modification of direct-FE method for nonlinear seismic analysis of arch dam-reservoir-foundation system considering spatially varying ground motion. Soil Dynamics and Earthquake Engineering. 2021;140:106477. https://doi.org/10.1016/j.soildyn.2020.106477
38. Mirzabozorg H, Varmazyari M, Gharehbaghi SA. Seismic evaluation of existing arch dams and massed foundation effects. Soils and Foundations. 2016;56(1):19-32. https://doi.org/10.1016/j.sandf.2016.01.002
39. Arjmandi SA, Lotfi V. Comparison of three efficient methods for computing mode shapes of fluid-structure interaction systems. Arabian Journal for Science and Engineering. 2013;38:787-803. https://doi.org/10.1007/s13369-012-0523-8
40. Willam KJ, editor Constitutive model for the triaxial behavior of concrete. IABSE Seminar on Concrete Structure subjected Triaxial Stresses; 1974.
41. Hanindya K, Makrup L, Paulus R. Deterministic Seismic Hazard Analysis to Determine Liquefaction Potential Due to Earthquake. Civil Engineering Journal. 2023;9(5):1203-16. https://10.28991/CEJ-2023-09-05-012

Persian Abstract

چکیده

سدهای بتنی به دلیل لایه‌های بتن‌ریزی به صورت ناهمسانگرد می‌باشد و این موضوع بر عملکرد آن‌ها تاثیر می‌گذارد. در این پژوهش با در نظر گرفتن تاثیر ناهمسانگردی ناشی از لایه‌های بتن‌ریزی، رفتار لرزه‌ای سد بتنی وزنی مطالعه شده است و پاسخ حالت‌های ایزوتروپیک و ارتوتروپیک مقایسه شده است. علاوه بر این در محدوده نرخ بارگذاری لرزه‌ای، با اعمال اثرات واقعی نرخ کرنش بررسی دقیق تری صورت گرفته است. سد بتنی وزنی کوینا به عنوان مطالعه موردی انتخاب شده است. نتایج نشان می‌دهد که ناهمسانگردی بتن منجر به جابجایی‌های دینامیکی بزرگ‌تر و سطح آسیب بیشتر در بدنه سد می‌شود. و در نظر گرفتن خواص ارتوتروپیک بتن سبب نتایج واقعی تر می شود. بیشینه تنش‌های کششی و فشاری نیز در مدل ناهمسانگرد نسبت به مدل همگن و ایزوتروپ افزایش می‌یابد که نشان می‌دهد در نظر گرفتن رفتار ارتوتروپیک بتن در آنالیز لرزه‌ای مفید می‌باشد. همچنین در نظر گرفتن نرخ کرنش در محدوده بارگذاری لرزه‌ای تفاوت آشکاری در نتایج ایجاد نمی‌کند. پس در نظر گرفتن ضرایب افزایش دینامیکی بالا در آنالیزهای عددی با خطا همراه است.